Probing athletics tracks degradation using a microscratch technique

Luca Andena[1,2*], Stefano Tagliabue[1], Andrea Pavan[1],

Andrea Marenghi[3], Manuel Testa[3], Roberto Frassine[1]

[1] Politecnico di Milano, Dipartimento di Chimica, Materiali e Ingegneria Chimica "Giulio Natta", Piazza L. Da Vinci, 32, Milano (Italy)

[2] Politecnico di Milano, Engineering, Exercise, Environment, Equipment for Sport (E4Sport) Lab, Piazza L. Da Vinci, 32, Milano (Italy)

[3] Mondo S.p.A., Piazzale Edmondo Stroppiana, 1, Alba (Italy)

* Corresponding author:
Luca Andena
Assistant Professor
Polymer Engineering Lab
Engineering, Exercise, Environment, Equipment for Sport Lab
Dipartimento di Chimica, Materiali e Ingegneria Chimica "G. Natta"
Politecnico di Milano
Piazza Leonardo da Vinci, 32 - 20133 Milano (Italy)
e-mail luca.andena@polimi.it
web https://www.cmic.polimi.it/dipartimento/ricerca/gruppi-di-ricerca/polyenglab-laboratorio-di-ingegneria-dei-polimeri/
tel +39 02 2399 3289
fax +39 02 2399 3280
ORCID 0000-0001-8610-1782

Abstract

Continuous outdoor exposure of athletics tracks can lead to an important degradation of their mechanical and aesthetical properties. In this work, flat laboratory samples prepared from rubber blends of different colours were subjected to natural and artificial ageing, to investigate their effect on the surface properties. Compositional variations demonstrated a generalized oxidization of the outer (top) material layer, together with surfacing of inorganic additives; a small increase of the degradation temperature of the natural rubber component was reported, similar to the one previously observed on bulk track samples. The smooth surface of the present samples allowed their testing using a microscratching technique, able to mechanically probe the material within a few hundred microns below the top surface. The formation of a significantly harder outer crust layer was reported, potentially impacting the track performance since it is exactly the locus of interaction between the athlete and the sport surface. In particular, the increase in scratch hardness is accompanied by a significant reduction in the apparent friction coefficient. These surface modifications, previously unreported in the literature, are independent phenomena with respect to generalized bulk ageing. Microscratch data supported by microscopy evidenced a significantly varying sensitivity to ageing for the different colours (red, blue, green, neutral). Moreover, this sensitivity appeared strongly dependent on the applied ageing protocol (natural vs. artificial). In view of these results, care must be taken when accelerated artificial weathering is used to simulate long-term natural ageing of these materials.

Keywords

1. Introduction and aim of the work

Athletic tracks made of synthetic materials have long replaced their natural counterparts in high-level competitions worldwide. Nowadays, multi-layered tracks made of complex rubber mixtures are used to grant the desired properties, required to ensure that athletes could safely perform sports activities to the best of their capacity. The International Association of Athletics Federations (IAAF) recommends their use and provides detailed guidelines regarding track construction [1] and approval [2-3].

Several factors affect the final behaviour of sports surfaces, including composition, geometrical structure and arrangement of their constituting layers [4-6]. The complex interplay between these variables prompted the development of numerical models as a tool to understand the behaviour of sports surfaces, predict their performance and allow their optimization [7-9]. With the help of these models, the separate effects of geometry and material properties were identified [10-13]; now we know that shock absorption is mostly determined by the elastic characteristics of the track material, together with its thickness. On the other hand, energy return [14] is also influenced by the dissipative properties of the material, which so far – to the authors' knowledge – have not been investigated in as much detail.

The preference expressed by IAAF for synthetic systems is not only because of their superior dynamic characteristics, but also because they require minimal maintenance - compared to the surfacing systems they have displaced [1]. However, information regarding the change in properties that synthetic tracks undergo over extended periods of time is lacking, with very few papers covering this subject [15]. This might be partially due to the quite complex nature of these systems which are frequently constituted by a blend of different rubbers, including large amounts of many additives. While ageing phenomena of rubbers in general have been studied in the past (e.g. [16-19]), the applicability of these findings to athletics tracks has not been demonstrated. On the other hand, the cost of field installations - which may vary considerably depending on their location and usage - makes their durability an aspect of crucial importance.

In a previous paper [20], the authors made a first attempt at identifying the physical phenomena occurring during track ageing and the variables affecting them – among which exposure to UV radiation was reported to play a very important role. As a result of that investigation, accelerated ageing protocols were developed and a few experimental techniques were singled out to monitor the evolution of track ageing with time. In particular, uniaxial compression testing and thermogravimetric analysis were found to be very effective for this purpose. However, the former only gives information on the track bulk, as the outcome of the test is determined by the average properties through the thickness of the track sample. The same study by Tagliabue et al. [20] also provided some evidence of the fact that specific degradation phenomena can affect the track surface, which is the part which athletes directly interact with. For this reason, taking inspiration from other studies in which surface mechanical probing was used to investigate degradation phenomena [21-23], surface microscratch testing was used in the present study to characterize the degradation evolution of several track formulations subjected to natural and artificial ageing.

2. Materials

Laboratory samples, specifically prepared for this work, were supplied by MONDO SpA, Alba (CN, Italy). All samples had the same polymeric composition irrespective of colour, at variance with commercial track products. The base blend consisted of natural rubber (NR) and styrene-butadiene rubber (SBR), with a small amount of ethylene-propylene-diene monomer rubber (EPDM) to improve weathering resistance. Some additives normally used to produce the top finishing layer of athletics tracks were also included in the blend: a paraffinic plasticizer, inorganic kaolin and anti-ozone protective wax.

The samples were compression moulded in the form of sheets and vulcanized at a temperature of 170 °C. While the adopted processing conditions were similar to those employed in the manufacture of commercial athletic tracks, the different geometry (in particular reduced thickness and the single layer) of the samples implies that they had likely different final properties. However, this

production route was necessary to obtain samples having a flat surface, apt to be submitted to microscratch testing: as a matter of fact, the anti-slip pattern present on real tracks prevents the execution of scratch tests on commercial track products.

Samples were prepared in four different colours: red (with iron oxides), blue (with phthalocyanine and titanium oxide), green (with phthalocyanine and chromium oxide) and neutral (with no added colour pigment; it naturally comes with a light brown hue). For each colour, 16 sheets measuring 250x200x4 mm were prepared for the natural ageing tests while one smaller sheet, of nominal dimensions 150x70x4 mm, had to be used for artificial ageing in view of the limited size of the environmental chamber used.

3. Experimental methods

Energy dispersive spectrometry, thermogravimetric analysis and scratch testing were performed on samples of the four different colours subjected to different ageing treatments, namely: no ageing (i.e samples as received), 1000h of artificial ageing, and 6, 12, 18 and 24 months of natural ageing. Naturally aged samples were also examined by optical and scanning electron microscopy.

3.1 Ageing protocols

The following two distinct ageing protocols were used in this investigation:

- **Artificial ageing**: samples were put in a dry environmental chamber and continuously irradiated for 1000 hours with a *Suga SX75 Super Xenon weather meter*, producing a specific power of 180 W/m² in the wavelength range between 300 and 400 nm. This level of irradiance is approximately three times higher than that of solar ultraviolet. The temperature during artificial ageing was maintained between 50 and 95°C.

- **Natural ageing**: samples were exposed to natural sunlight in the Q-Lab weathering facility in Buckeye (AZ, USA) according to the ASTM G7-13 Arizona test method [24]; they were subsequently collected after exposure times of 6, 12, 18 and 24 months.

Figure 1 shows the surface of samples of the four different colours observed at different stages. The images were acquired using a commercial flatbed scanner (*Epson Perfection V33*) with a resolution of 240 dpi and a colour depth of 24 bit. Heavy discoloration is evident in the artificially aged samples while the ones subjected to natural ageing do not differ much from unaged ones if not for a slightly darker hue observed on some samples. The appearance of the 18-month samples differs slightly from that of the rest of the naturally aged ones. This difference could be related to some unknown operations performed during exposure at the weathering site. However, as no changes in trends measured with the following techniques were reported over time, this minor difference was ignored.
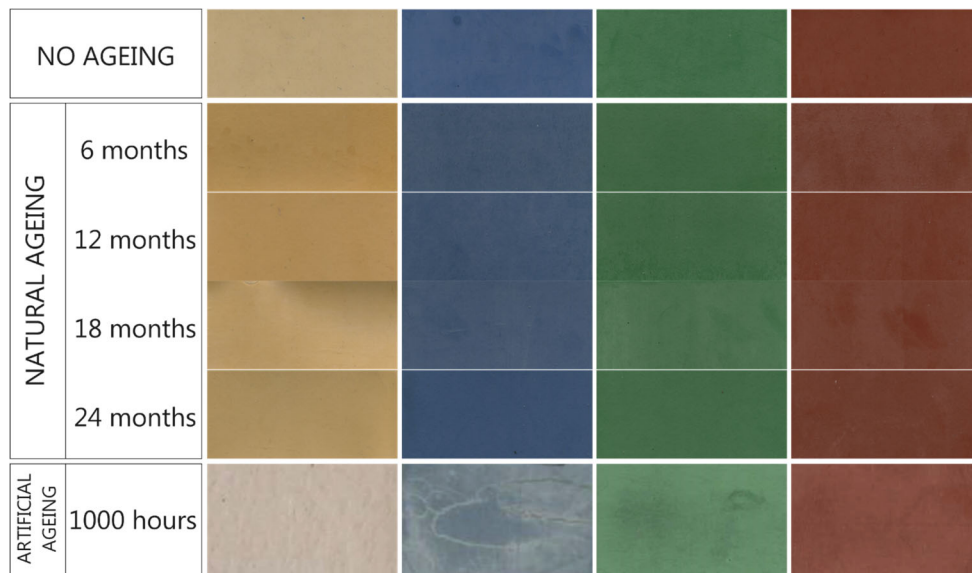
Figure 1. Surfaces of track samples in the four colours, as acquired with a commercial flatbed scanner. From left to right: neutral, blue, green, red samples; ageing times are indicated on the left. (For a better appreciation of the variations in colours in this figures, the reader is referred to the web version of this article).

3.2 Energy dispersive spectrometry (EDS)

Both unaged and aged samples were analysed using scanning electron microscopy (*Zeiss Evo 50 EP*). Energy dispersive spectroscopy was carried out to quantitatively measure the relative amount of given elements at the surface of the samples. In particular, elements C, O, Al and Si were considered for all the colours, in accordance with the analysis presented in [20]. In addition, the presence of inorganic fillers, specific for each colour, was tracked in different samples; in particular:

- titanium in the blue samples

- chromium in the green samples

- iron in the red samples

At variance with the previously mentioned study, EDS results are fully quantitative thanks to the surface homogeneity of the samples used in the present study (in contrast with the surface of real track samples). Carbon and oxygen represent the organic part of the material and its oxidation; Al and Si in turn are relevant to the inorganic filler component present in all the rubber mixtures. A relative increase observed in the specific inorganic filler signal was attributed to degradation of the relevant organic matrix.

3.3 Thermogravimetric analysis (TGA)

Thermal degradation of the track constituent materials was investigated by means of a *TA Instruments TGA Q500 analyser* on small specimens (30 to 40 mg) obtained from the samples' surface. Two specimens for each colour at each ageing stage, starting from the unaged ones, were tested. The same thermal program proposed in [20], composed of the following stages (starting from a nitrogen atmosphere), was adopted in the present study:
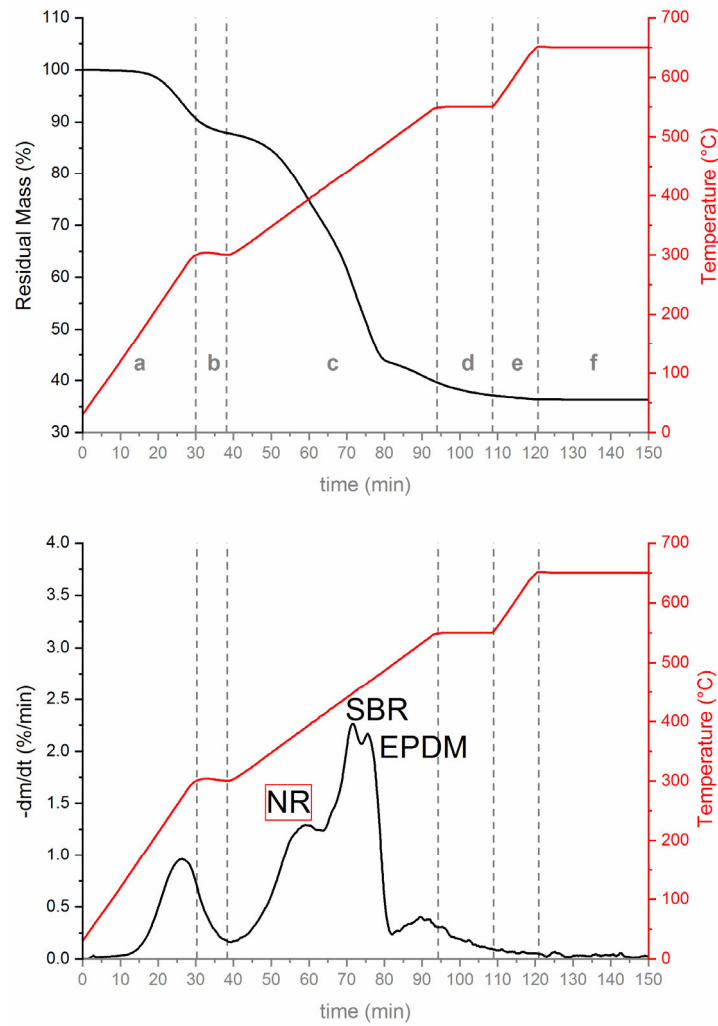
Figure 2. Typical temperature program (in red) and measurements (in black) obtained from TGA of the samples studied in this work: residual mass (upper plot) and its derivative with time (lower plot). Peaks are labelled according to the individual constituents of the rubber mixture; NR's one is highlighted since it is considered to monitor the ageing process, as reported in [20]. Data shown are for an unaged red sample.

a. Heating from 25 to 300 °C at 10 °C min^{-1}

b. Holding at 300 °C for 10 min

c. Heating from 300 to 550 °C at 5 °C min^{-1}

d. Holding at 550 °C for 15 min

e. Heating from 550 to 650 °C at 10 °C min^{-1}

f. Switch to standard air atmosphere and holding at 650°C for 30 min

Specimen mass, m, was continuously recorded and the residual mass was normalized (as % of the original mass) and differentiated with respect to time to more easily identify peaks associated to degradation of individual constituents of the rubber mixtures (NR, SBR, EPDM), as shown in

Figure 2. In accordance with the findings reported in [20], the variation of the NR degradation peak temperature with ageing was closely monitored as a good indication of rubber matrix degradation.

3.4 Scratch test

Tests were run on a *CSM Microscratch* tester equipped with a sphero-conical diamond indenter, having a 90° apex angle and a 200 μm radius tip. Small specimens cut from the sheet samples were glued on a thick, rigid, glass-fibre reinforced polyethylene substrate. Scratches were then introduced with the indenting stylus sliding at a relative speed v = 20 mm/min according to two different testing protocols:

- **Continuously increasing load**: during preliminary tests the normal load, F, was increased linearly from 0 to 1.5 N over a scratching distance x = 2 mm; these tests were only performed on the artificially aged samples and the 6 months naturally aged ones

- **Stepwise increasing load**: in the following series of tests the scratch was performed with an increase of F by steps of 0.3 N, starting from 0.6 N up to at least 1.5 N (depending on the maximum penetration depth reached during the analysis, which was limited to 500 μm).

  Each step (occurring at constant normal load F) was prolonged over a distance x = 2 mm.

The adopted testing configuration together with the typical outcome of scratch experiments conducted according to the two testing protocols is displayed in Figure 3.
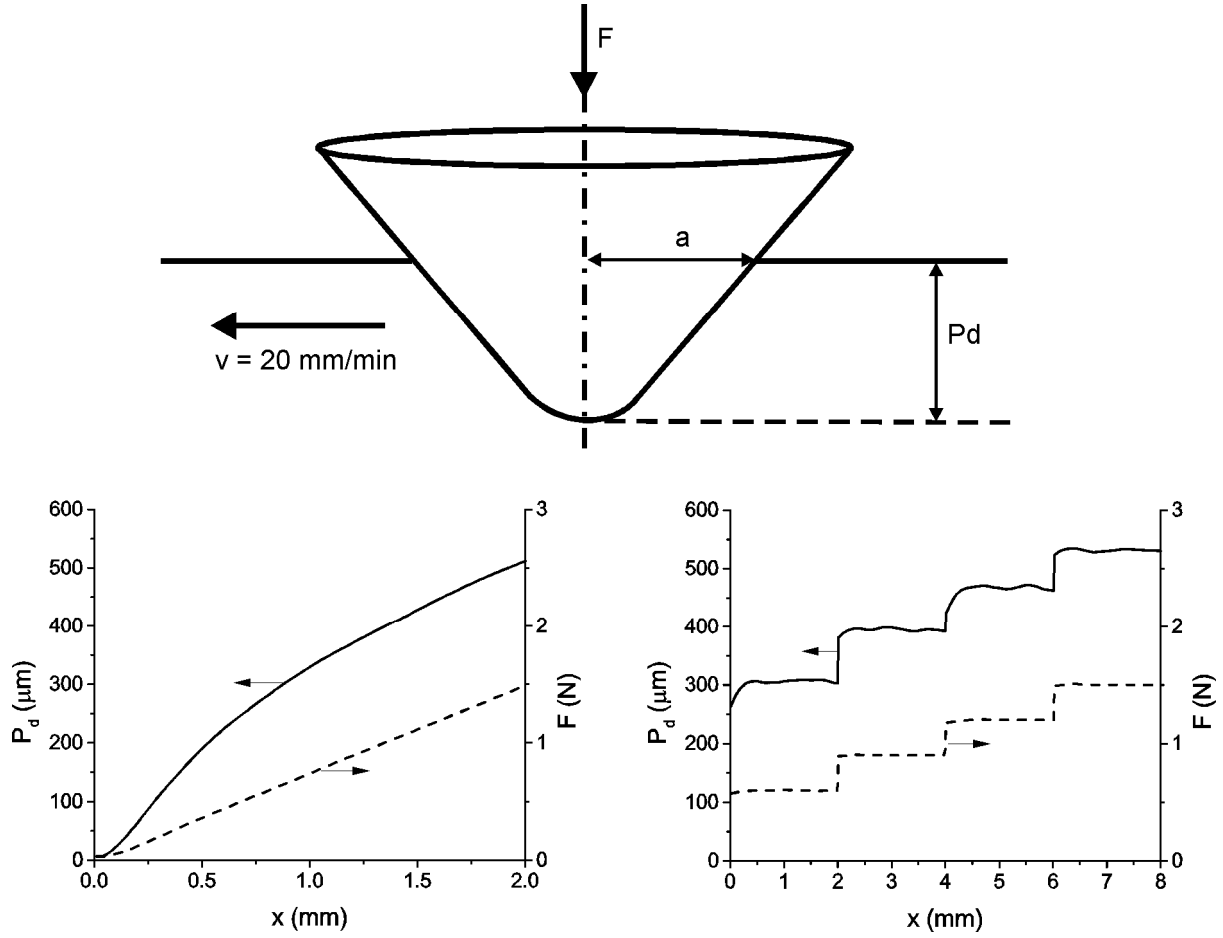
Figure 3. Top) scratch test configuration: F – normal load; v – scratching speed; P_d – penetration depth; a – contact radius. Bottom) Example of penetration depth data (solid lines) and corresponding applied load (dashed lines) vs. scratch distance for the unaged red material, according to the two testing protocols: continuously increasing load (left) and stepwise increasing load (right).

The penetration depth, P_d, and tangential force opposing motion, F_t, were measured during all the tests; for each condition, at least three repetitions were made and results were averaged.

An apparent coefficient of friction μ was calculated using equation 1:

$$\mu = \frac{F_t}{F} \qquad (1)$$

It is named 'apparent' as it also depends on the particular geometry (shape and size) of the indenter. For the stepwise increasing load protocol, an apparent value of the scratch hardness [25-26], H, was also evaluated for each load level according to equation 2:

$$H = q\frac{F}{\pi a^2} \qquad (2)$$

where F is the normal load, a is the contact radius and q is a material dependent parameter whose value was set to 1, according to the assumption of a purely elastic nature of the contact between

10

indenter and rubber samples. This assumption is in accordance with the very small residual depth measured after scratch testing (significantly less than 10%). The contact radius a was evaluated following purely geometrical considerations as per equation 3:

$$\begin{cases} a = \sqrt{2RP_d - P_d^2} & if\ P_d < 59\ \mu m \\ a = P_d + R(\sqrt{2} - 1) & if\ P_d > 59\ \mu m \end{cases} \tag{3}$$

The value of 59 μm identifies the depth at which the transition between the spherical tip and the conical part of the indenter occurs for the specific geometry used.

3.5 Optical and electron microscopy

To observe possible surface changes brought about by the ageing processes in detail, small specimens to be examined under optical and scanning electron microscopes were obtained via die cutting. For this purpose 12 and 24 month naturally aged samples were considered; some additional samples aged for 30 months under the same conditions that became available during this study were also analysed.

3.5.1 Optical Microscopy (OM)

The cut specimens were encapsulated in epoxy resin. They were then worked with a lapper and subsequently polished with SiC abrasive paper and then with diamond paste. Polishing operations were performed carefully at low speed to obtain a very flat surface while preventing sample heating. Analysis was made with an *Olympus BX-60* in reflectance polarized light configuration with a magnification level of 5x and 10x. Images were collected with an *Infinity 2 Camera* and then processed with *ImageJ 1.52* software to perform dimensional measurements.

3.5.2 Scanning Electron Microscopy (SEM)

Specimens to be observed under SEM were sputtered with a thin gold layer to increase their electrical conductivity. Surfaces were observed with *SEM Zeiss Evo 50 EP* in high vacuum configuration at different magnification levels (75x, 100x and 500x). Micrographs were analysed with *ImageJ 1.52* software and results compared with those obtained via optical microscopy.

4. Results and discussion

Figure 4 shows the variations of the composition of the samples as measured by EDS, as a function of ageing time. For all samples there is a very high initial C content, due to the presence of a wax anti-ozone protective surface layer. After the first natural ageing step, a marked decrease of C, with an opposite variation of O, was observed. This trend is compatible with significant oxidization of the outermost surface layer (within a thickness of 10 nm, therefore not relevant even for microscratch tests). The relative content of C and O remains stable in the subsequent steps.

In the same timeframe also Si and Al signals appear, probably related to the surfacing of the inorganic fillers after the polymeric matrix or its organic additives (such as the anti-ozone protective layer) are partially removed by degradation. This interpretation is supported by the observation that, in the case of the coloured samples, also the signals of Ti, Cr and Fe, whose oxides correspond to the colours of blue, green and red samples, respectively, appear after the 6 months period of marked degradation. As for the artificial ageing, results are qualitatively similar but with a more severe oxidative effect of the 1000h treatment, compared with 24 months of natural ageing; the only exception is for the red coloured sample, whose results are quite similar for both ageing protocols. This difference is a first evidence that the two ageing processes (natural and artificial) are not equivalent.
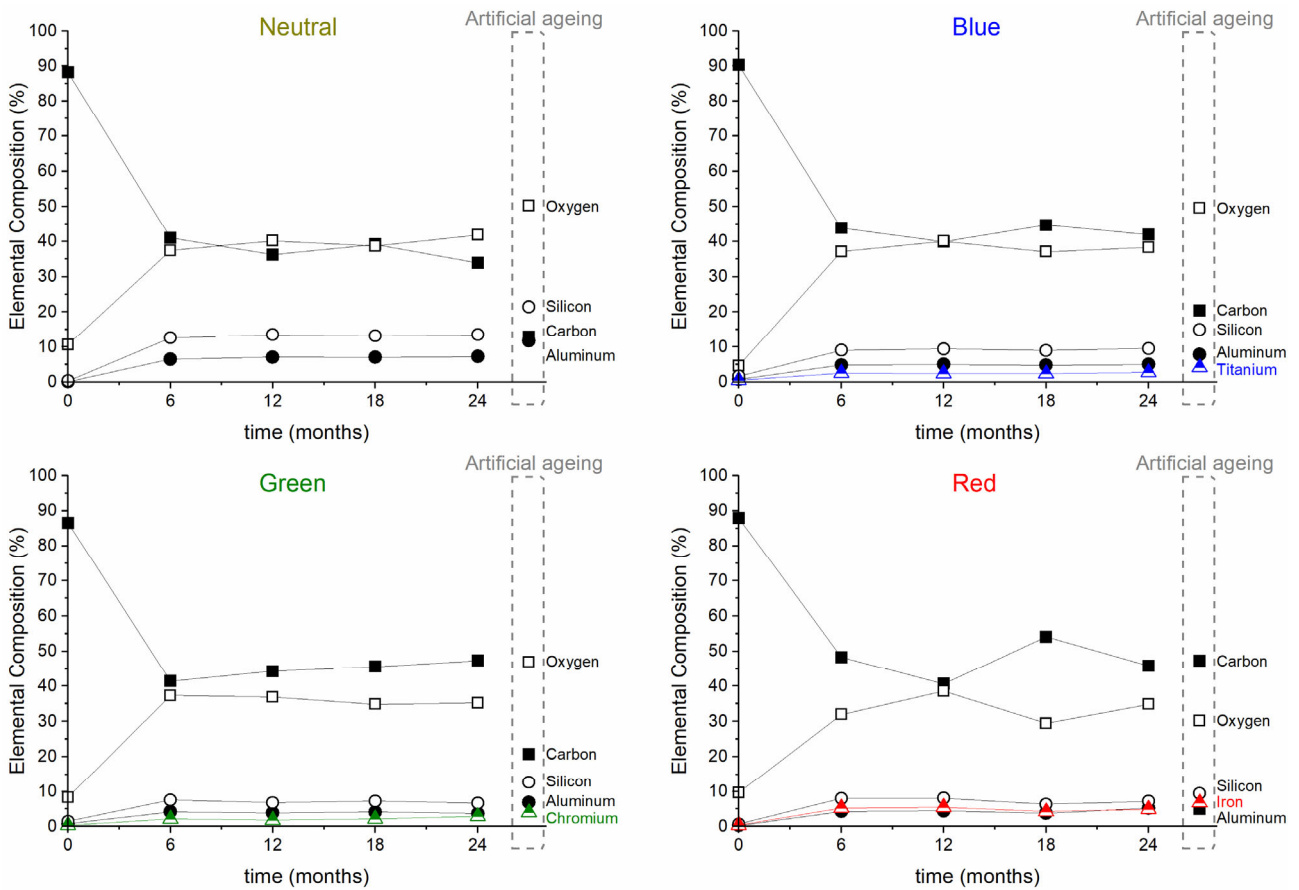
Figure 4. Sample composition as given by EDS measurements as a function of natural ageing time for samples of the four colours. Relevant data from artificially aged samples are shown on the right of each graph (enclosed between dashed lines).

The evolution of the degradation temperature with ageing time in the NR component, as measured by TGA, is plotted in Figure 5. As already observed in [20], there is a moderate initial increase during the first 6 months period and a subsequent acceleration of the related phenomenon, with the degradation temperature reaching values about 5-10°C higher than the initial temperature of 370-375°C, after 24 months of natural ageing. In this case, the artificial ageing treatment produces smaller changes, comparable in general with those obtained during the first 6-12 months of natural ageing. Results are quite similar irrespective of the sample colour.
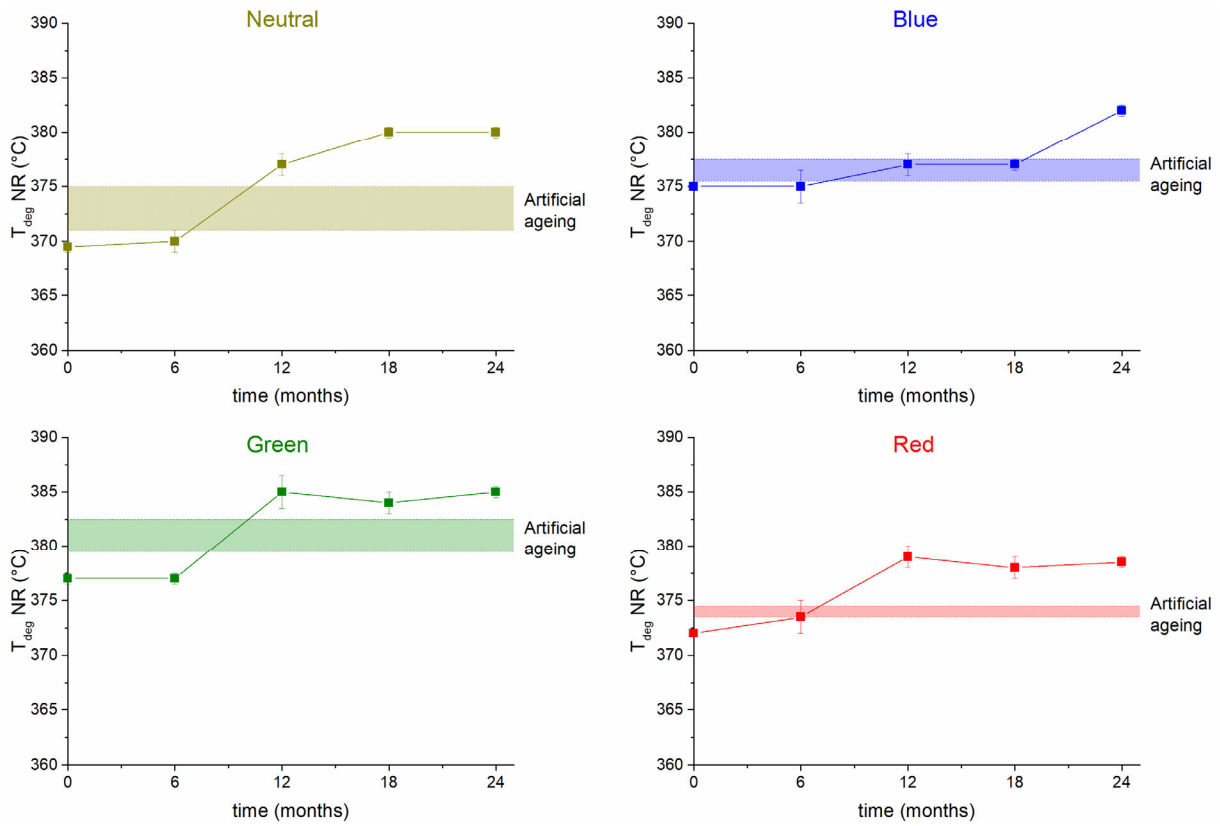
Figure 5. Degradation temperature of the NR component of the four samples as a function of natural ageing time, as measured by TGA; error bars represent the data dispersion of the 2 samples tested for each condition. Data from artificially aged samples is represented as a shaded band whose height represents the dispersion of the relevant TGA measurements.

After receiving the first set of samples, aged artificially for 1000 hours and naturally for 6 months, preliminary scratch tests were performed according to the continuously increasing load protocol described in section 3.4. Results are shown in Figure 6 as penetration depth vs. scratch distance curves, covering a normal load range from 0 to 1.5 N. Some interesting results can be drawn by comparing data for the different samples.
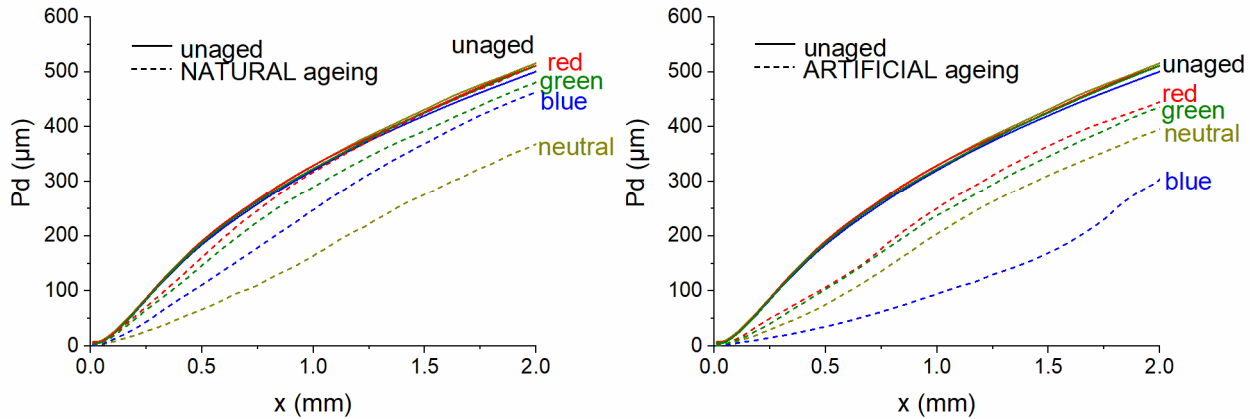
Figure 6. Penetration depth vs. scratch distance data under continuously increasing loading for unaged (solid lines) and aged (dashed lines) samples. The same reference curves obtained for the unaged samples (solid lines) are separately compared with the curves obtained for the 6 month naturally aged samples (left) and the 1000 hour artificially aged samples (right).

Firstly, all curves obtained for the unaged samples (solid lines in the graph) are almost identical, indicating that scratch resistance is initially equal, irrespective of the different colours. However, after a relatively short period of natural ageing, important differences already arise: while red samples are almost unaffected, the neutral ones display a considerably lower penetration depth at all levels of load, which indicates an increase in scratch hardness. Green and blue samples exhibit an intermediate behaviour. When considering artificially aged samples (graph on the right in Figure 6), the increase in hardness is even more evident. In this case the red samples and the green samples are much closer to the neutral ones but the most dramatic effect is the very large decrease of penetration depth (and corresponding increase in scratch hardness) observed for the blue samples.

The ability of scratch testing to mechanically probe the material close to the exposed surface (as opposed to bulk mechanical characterization in tensile or impact tests) makes this technique a useful tool to analyse the sensitivity to different ageing protocols.

To get a more quantitative evaluation of the results, stepwise increasing load was applied. Its advantage lies in the fact that – provided scratch length of a single step is large enough to attain steady state scratching conditions – an accurate evaluation of scratch hardness can be obtained via equation 2. A typical outcome of stepwise increasing loading scratch tests is reported in Figure 7.
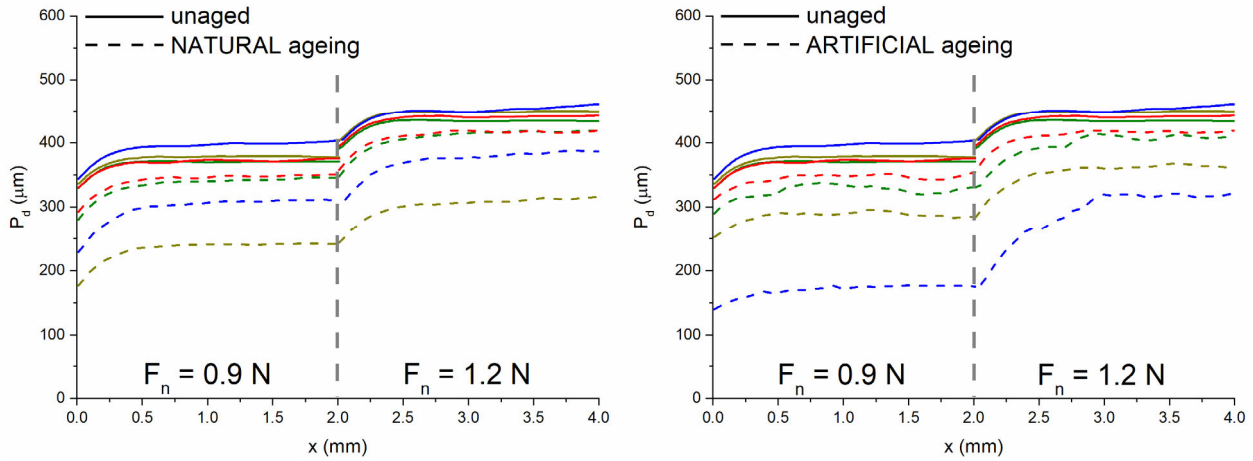
Figure 7. Penetration depth vs. scratch distance data under two different values of constant load (as indicated) for unaged (solid lines) and aged (dashed lines) samples. A comparison with the same unaged reference curves is separately made for naturally (6 months, left) and artificially (1000 hours, right) aged samples.

Results for all tested samples are shown in Figure 8, in which scratch hardness is plotted as a function of the relevant steady state penetration depth attained at each step of the stepwise increasing load scratch testing. It must be noted that, for each material/condition, P_d increases with increasing normal load, thus leading to a lower value of the scratch hardness, H. This means that, under higher load values, a larger volume of material is involved in determining the overall mechanical response which, of course, is related to an integral of the material behaviour over the thickness of material affected by the test.

Several trends can be identified. First of all, aged materials display a larger scratch hardness than the corresponding unaged ones: for natural ageing, this difference becomes larger with increasing ageing time. Moreover, the increase of H for naturally aged materials is more pronounced for smaller P_d values, i.e. at lower levels of applied normal load and correspondingly lower thicknesses of probed material. The same result can be observed for artificial ageing on the blue samples but not on the other colours: on the latter, tests were run with a very low normal load but they did not yield reliable results under these conditions.

With increasing load, the indenter penetration increases, and the calculated scratch hardness H tends to level off (though not to zero), but the corresponding plateau level is still influenced by ageing time.
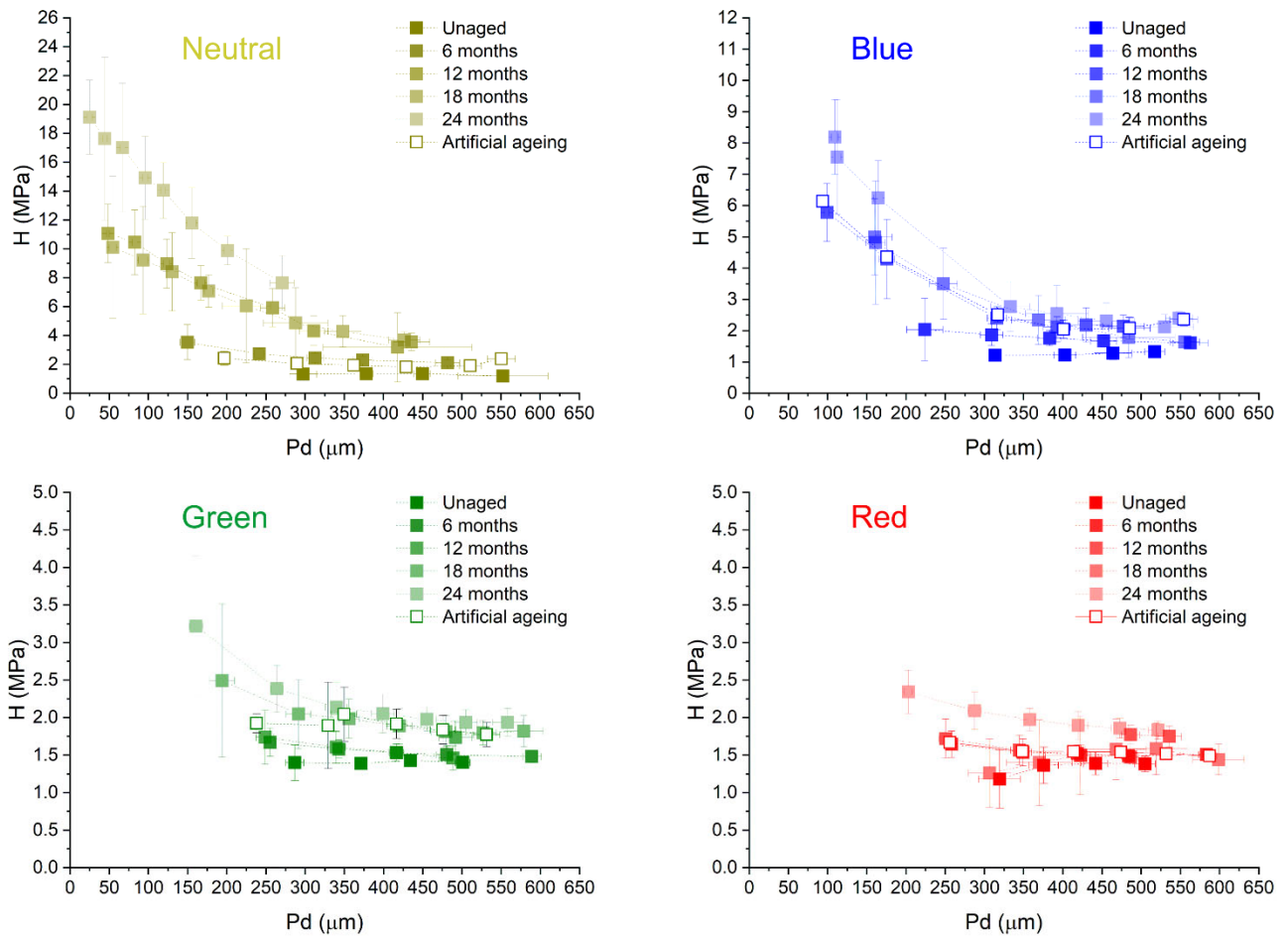
16

*Figure 8. Scratch hardness as a function of penetration depth for unaged and aged samples of different colours subjected to stepwise increasing load scratch testing with various normal loads. Error bars represent the dispersion of the experimental measurements. **Please note the different scales used**.*

Scratch testing results suggest that ageing brings about a twofold effect: (*i*) there is a general variation in mechanical properties with a moderate increase in scratch hardness, as already observed in the bulk of track samples analysed in [20] and (*ii*) a hard crust, with a characteristic thickness of about a hundred microns, grows on the exposed surface of the samples (more likely to be subjected to extensive material oxidation). The effect observed is qualitatively comparable with the findings reported in [19] for aged SBR with and without added TiO_2. The main mechanisms proposed therein are the formation of oxidised photo-products and related crosslinking, which appears to be predominant over chain scission.

Considering the different colours, the magnitude of the scratch hardness of the naturally aged samples increases considerably over the value of 1.5 MPa shown by unaged ones: depending on the applied load, higher values range from 2-3 MPa for red and green to 6-8 MPa for blue and up to 10-

20 MPa for neutral samples. This fact highlights the markedly different sensitivity of the different colour formulations to the crust formation phenomenon. As already mentioned, data for artificially aged samples could not be obtained for the range of P_d in which the crust formation can be observed, except for blue samples. Nevertheless, data seem to follow similar trends irrespective of the testing protocol (with relative values depending on the colour considered).

The increase in surface scratch hardness is associated to a dramatic reduction of the apparent coefficient of friction measured during scratch testing, as evident in the data displayed in Figure 9. The loss of frictional resistance by the surface is only observed when the value of H becomes significantly larger with respect to that of the relevant unaged surface: this clearly occurs for the green and the blue samples. After this phenomenon develops, the apparent coefficient of friction becomes relatively insensitive to ageing time, for a given scratch penetration depth. The whole picture is consistent with the formation of a hard superficial crust, whose surface properties are then relatively unaffected by subsequent ageing (although its thickness likely continues to grow).
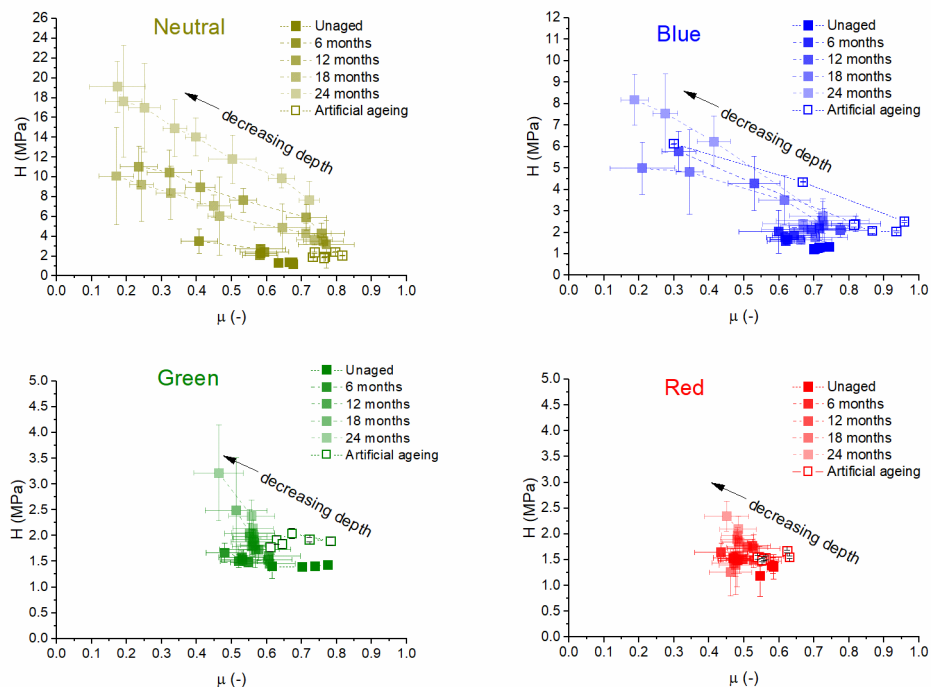

*Figure 9. Correlation between scratch hardness and apparent coefficient of friction for unaged and aged samples of different colours subjected to stepwise increasing load scratch testing with various normal loads. Error bars represent the dispersion of the experimental measurements. **Please note the different scales used**.*

To support microscratch results with direct evidence of the crust formation, its presence was identified by looking at the samples' cross-section with both optical and electron microscopy (Figures 10 and 11).
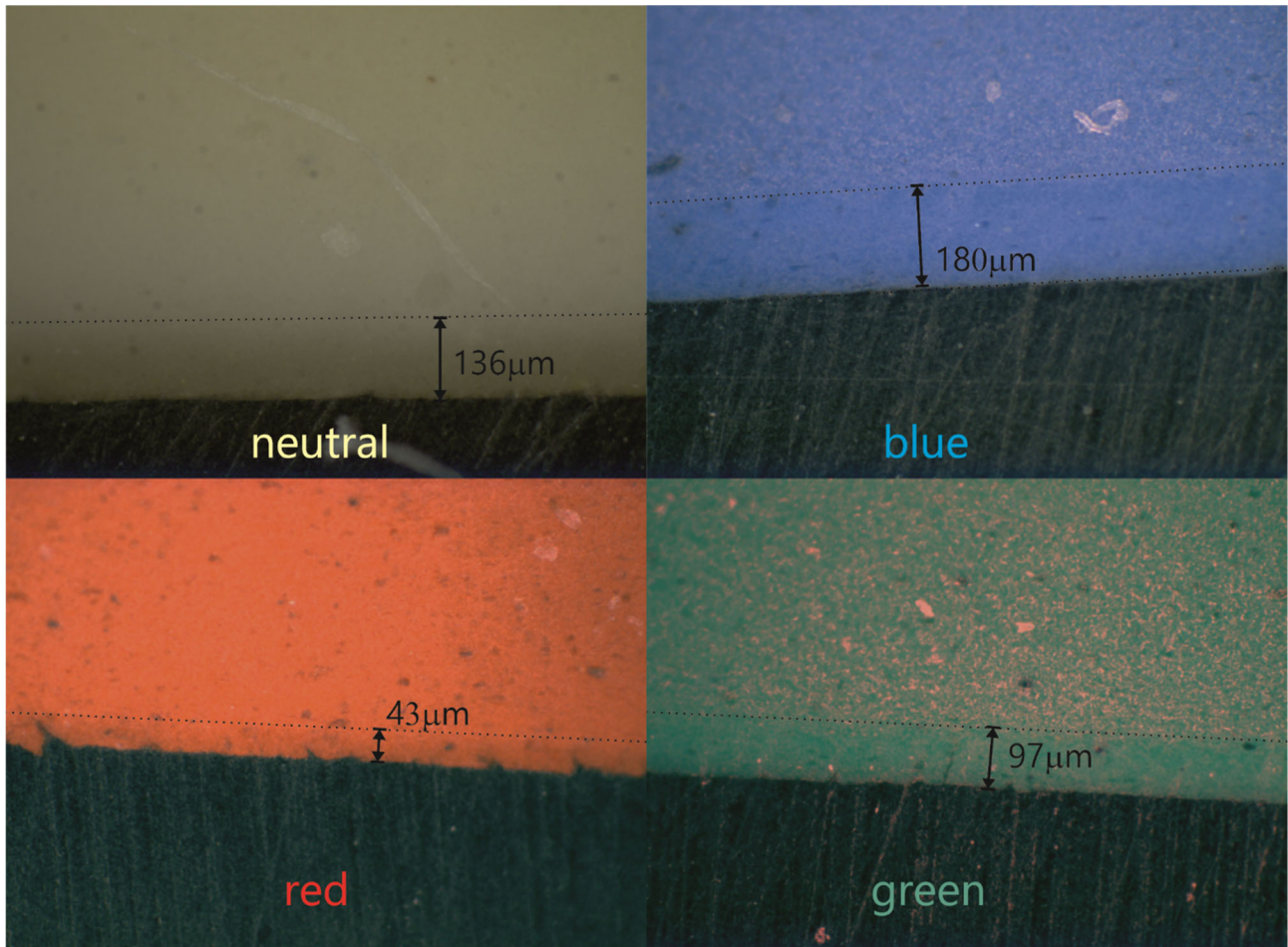
Figure 10. Optical micrographs of 30-month naturally aged samples at 10x magnification. Their cross-section is shown, with the exposed surface at the bottom of each picture. Details of the surface crust are shown together with the average value of its thickness, as it results from several measurements performed on each sample.
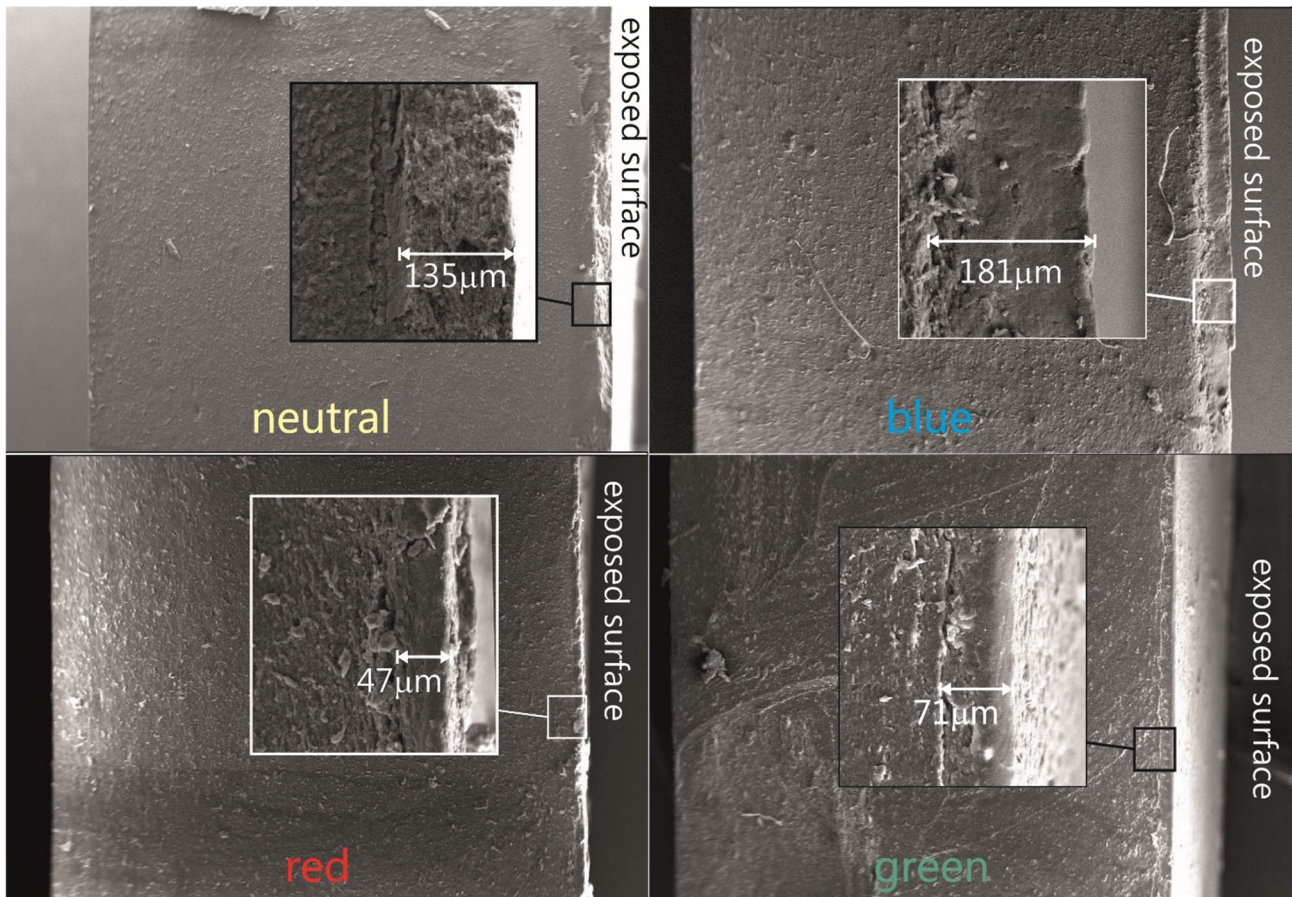
Figure 11. Electron micrographs of 30-month naturally aged samples (cross-section view) at 100x magnification. Insets at 500x magnification detail the surface crust and the results of relevant thickness measurements.

On the side of the exposed surface, a region with a distinctly different appearance from the bulk was actually detected for all materials. This difference was more evident in the scanning electron micrographs (SEM) than in the optical ones (OM). As mentioned in the experimental methods section, *ImageJ* software was used to perform several measurements of the thickness of this crust region. Crust thickness could be determined with reasonable accuracy, despite a certain level of uncertainty caused by poor contrast between the crust and the bulk, which hinders the identification of a clear boundary between them. Results of several measurements performed on each image (whether OM or SEM) were averaged and standard deviation was calculated: they are plotted in Figure 12.

The average values for any given colour (listed in Figures 10 and 11 for the 30-month ageing samples) are quite consistent between OM and SEM measurements, with the exception of the blue (12-month) and the red (24-month) for which we cannot provide a clear explanation. Given the

general agreement observed on the same materials for the other ageing times, we just suppose that the difference comes from the measurements of the crust thickness from the micrographs.
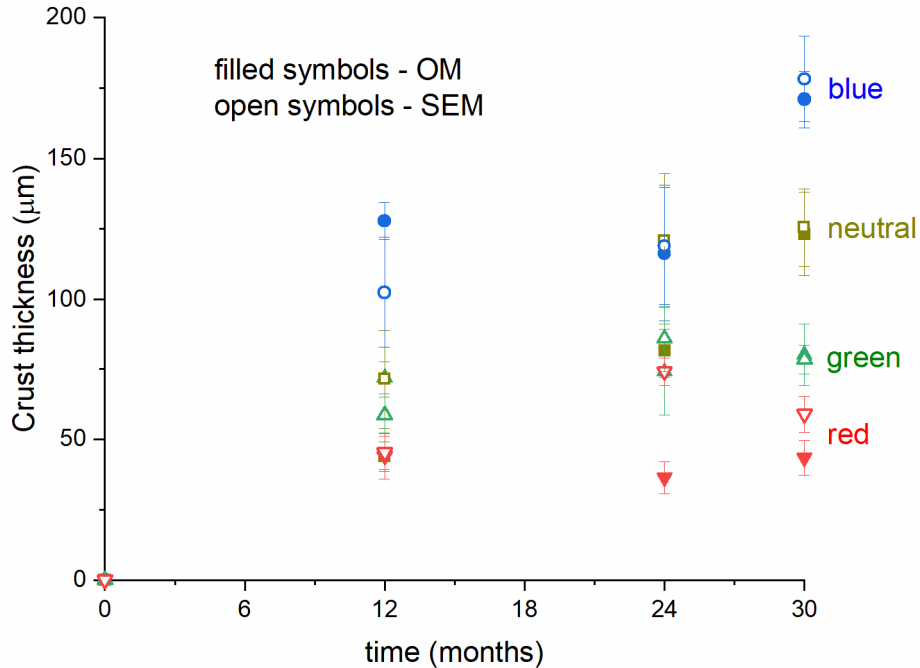

Figure 12. Comparison of average crust thickness measurements performed on optical (OM) and scanning electron (SEM) micrographs, as a function of natural ageing time. Error bars represent the standard deviation of the measurements.

Data in Figure 12 show that the crust grows to significantly larger thickness values in neutral and blue samples; in red and green samples, in turn, it grows much less and seems to level off after 12 months of exposure. A qualitative agreement with scratch hardness measurement can thus be found, although only to a certain extent: while a larger thickness was indeed expected for blue and neutral, data in Figure 8 would suggest a much larger sensitivity of the latter compared to the former. In fact, the opposite trend is observed. This would imply that the intrinsic quality of the crust could be different (i.e. harder for neutral samples) irrespective of its thickness.

A comparison between the results obtained with the two ageing protocols is shown in Figure 13 in which the H values of each naturally aged sample, $H_{Natural\ ageing}$, are normalized with respect to the H values of the corresponding (same colour) artificially aged samples, $H_{Artificial\ ageing}$, tested under the same normal load.
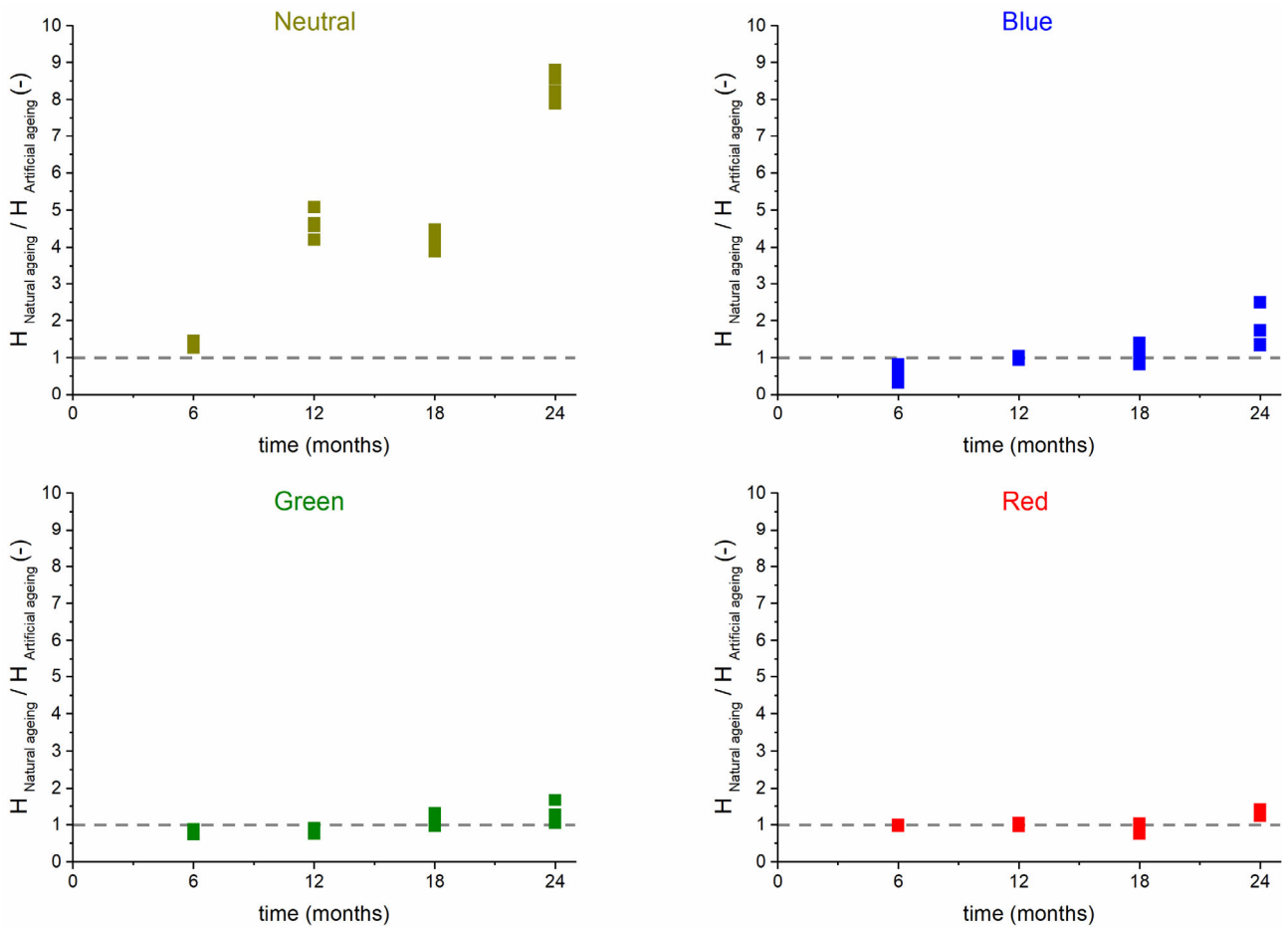
Figure 13. Relative scratch hardness of naturally aged samples shown as a function of natural ageing time (points) with respect to the hardness of the corresponding 1000h artificially aged samples (dashed line), tested under the same normal load

The dramatic effect of natural ageing on neutral (not pigmented) samples is clearly visible. After 6 months of exposure the scratch hardness is comparable to that of (1000h) artificially aged samples and then it increases considerably, of up to nearly an order of magnitude after 24 months.

The result is quite different with the coloured samples, for which a substantial equivalency between natural and artificial ageing is observed during the first 12-18 months of exposure, whereas a moderate increase in hardness of the naturally aged samples over that of the artificially aged ones is observed around 24 months. In the case of the red and green samples this late increase is quite modest, showing a diminished propension to the crust formation.

This set of results proves that the relative ageing resistance of samples having different colours is significantly affected by the specific ageing protocol used. The reason is likely related to the specific interaction of inorganic pigments (basically made by oxides of Cr for green, Ti for blue and

Fe for red) with the incoming UV radiation having different wavelength and intensity characteristics. As a consequence, caution should be taken when using artificial ageing to perform accelerated weathering testing since the obtained results might not be representative of the actual in-field behaviour of the track products. Moreover, maintenance treatments (involving brushing) performed on installed track fields might interfere with crust formation, thus leading to some variations in material scratch hardness with respect to what was observed in the lab.

As a general remark, alterations of the thin outermost surface layer of the track may not have a great impact on the overall mechanical behaviour of the track (e.g. its shock absorption characteristics), but they significantly influence other surface-related properties such as friction [27] (which can considerably impact the athlete's traction), besides having an obvious effect on visual appearance.

5. Conclusions

In this work the ageing of materials typically used for the production of athletics tracks of different colours (red, green, blue and unpigmented neutral) was investigated. Flat laboratory samples having a formulation similar to what is used for actual tracks were subjected to natural ageing for 6, 12, 18 and 24 months and to accelerated artificial ageing for 1000h. This choice of samples allowed the use of techniques (such as quantitative EDS and microscratch) not applicable on track products, because of their relatively rough surface texture (a feature that is necessary to ensure sufficient traction to the athletes). These techniques were coupled with TGA and microscopy (electron and optical), which *per se* can be used on both type of samples.

EDS demonstrated the occurrence of surface ageing-related oxidation phenomena and highlighted by surfacing of mineral pigments added to the polymeric formulations of different colours. Ageing was also detected via TGA by monitoring the increase of the degradation temperature of the NR component, as already suggested by a previous study.

The main outcome of this investigation was the successful application of microscratch testing to mechanically probe the sample surface (to a depth of a few hundred microns) and relate the results

to ageing. Besides confirming the stiffening effect generally observed within the bulk material, already identified in previous investigations, microscratch testing allowed the recognition of a previously unreported phenomenon: the formation of a hard crust at the sample surface, whose scratch hardness is quite sensitive to the material colour. In particular, unpigmented samples showed an almost tenfold hardness increase (compared to the unaged material) after exposure to natural ageing, while red and green ones were only slightly affected; blue samples displayed an intermediate behaviour.

Evidence of crust formation on the top surface of the samples exposed to natural ageing was given by optical and electron microscopy analyses, which gave relatively consistent results and allowed to monitor crust growth as a function of ageing time. Crust thickness measurements confirmed that red and green samples were less affected than blue and neutral ones, but the relative behaviour of these latter two did not match scratch hardness measurements. This would suggest that crust properties may sensibly vary for the different colours.

Results from artificially aged samples were similar but some important differences with respect to natural ageing were found, in particular with a high sensitivity reported for the blue colour. This fact should lead to a certain degree of caution when using accelerated artificial ageing to characterize the weathering resistance of the kind of rubber blends athletics tracks are made of: results may be not fully consistent with the expected performance in the field.

A final observation concerns the frictional properties of aged surfaces: as soon as a significant increase in scratch hardness occurs, a very large reduction in the apparent friction coefficient appears. It is to note that these findings were obtained on laboratory specimens aged under harsh conditions. The actual performance experienced by running athletes on a typical, well-maintained embossed track will likely be impacted less severely; nonetheless, any development of the track's formulation aimed at suppressing crust formation is expected to be highly beneficial in this regard.

Acknowledgements

Data availability

The raw data required to reproduce these findings cannot be shared at this time due to technical or time limitations. The processed data required to reproduce these findings are available to download from Mendeley Data.

REFERENCES

1. IAAF Track and Field Manual, 2008.
2. EN 14808 Surfaces for sports areas - Determination of shock absorption.
3. EN 14809 Surfaces for sports areas - Determination of vertical deformation.
4. G. Baroud, B.M. Nigg, D.J. Stefanyshyn, Energy storage and return in sport surfaces, Sports Eng. 2 (1999) 173.
5. J.V. Durà, A.C. Garcìa, J. Solaz, Testing shock absorbing materials: the application of a viscoelastic linear model, Sports Eng. 5 (2002) 9.
6. M. Benanti, L. Andena, F. Briatico-Vangosa, A. Pavan, Viscoelastic behavior of athletics track surfaces in relation to their force reduction, Polym. Test. 32 (2013) 52.
7. R.D. Thomson, A.E. Birkbeck, T.D. Lucas, Hyperelastic modelling of nonlinear running surfaces, Sports Eng. 4 (2001) 215.
8. M.J. Carré, D.M. James, S.J. Haake, Hybrid method for assessing the performance of sports surfaces during ball impacts, Proc. Inst. Mech. Eng. Part L: J. Mat Des Appl 220 (2006) 31.
9. L. Andena, F. Briatico-Vangosa, A. Ciancio, A. Pavan, A finite element model for the prediction of Force Reduction of athletics tracks, Proc. Eng. 72 (2014) 847.
10. L. Andena, F. Briatico-Vangosa, E. Cazzoni, A. Ciancio, S. Mariani, A. Pavan, Modeling of shock absorption in athletics track surfaces, Sports Eng. 18 (2015) 1.
11. L. Andena, S. Aleo, F. Caimmi, S. Mariani, F. Briatico-Vangosa, A. Pavan, A 3D Numerical Model for the Optimization of Running Tracks Performance, Proc. Eng. 147 (2016) 854.
12. D. Cole, S. Forrester, P. Fleming, Mechanical Characterisation and Modelling of Elastomeric Shockpads, Appl. Sci. 8 (2018) 501.
13. L. Andena, S. Aleo, F. Caimmi, F. Briatico-Vangosa, S. Mariani, S. Tagliabue, A. Pavan, Modelling the cushioning properties of athletic tracks, Sports Eng. 21 (2018) 453.
14. L. Andena, A. Ciancio, F. Briatico-Vangosa, S. Mariani, A. Pavan. On the relationship between force reduction, loading rate and energy absorption of athletics tracks, Proc. Inst. Mech. Eng. Part P J. Sports Eng. Tech. 232 (2018) 71.

15. V. Wachtendorf, U. Kalbe, O. Krüger, N. Bandow. Influence of weathering on the leaching behaviour of zinc and PAH from synthetic sports surfaces, Polym. Test. 63 (2017) 621–631.
16. C. Adam, J. Lacoste, J. Lemaire. Photo-oxidation of elastomeric materials. Part 1—Photo-oxidation of polybutadienes, Polym. Deg. Stab., 24 (1989) 185
17. C. Adam, J. Lacoste, J. Lemaire. Photo-oxidation of elastomeric materials: Part II—photo-oxidation of styrene-butadiene copolymer, Polym. Deg. Stab., 26 (1989) 269
18. M.Celina, J.Wise, D.K.Ottesen, K.T.Gillen, R.L.Clough. Oxidation profiles of thermally aged nitrile rubber, Polym. Deg. Stab. 60 (1998) 493.
19. G. Mertz, F. Hassouna, P. Leclère, A. Dahoun, V. Toniazzo, D. Ruch. Correlation between (nano)-mechanical and chemical changes occurring during photo-oxidation of filled vulcanised styrene butadiene rubber (SBR), Polym. Deg. Stab. 97 (2012) 2195.
20. S. Tagliabue, L. Andena, A. Pavan, A. Marenghi, E. Testa, R. Frassine. Ageing in athletics tracks: A multi-technique experimental investigation, Polym. Test. 69 (2018) 293.
21. M. Contino, L. Andena, M. Rink, A. Colombo, G. Marra. Fracture of high-density polyethylene used for bleach bottles, Proc. Struct. Int. 2 (2016) 213.
22. D. Saviello, L. Andena, D. Gastaldi, L. Toniolo, S. Goidanich. Multi-analytical approach for the morphological, molecular, and mechanical characterization after photo-oxidation of polymers used in artworks, J. App. Polym. Sci. 135 (2018) 46194.
23. M. Contino, L. Andena, M. Rink, G. Marra, S. Resta. Time-temperature equivalence in environmental stress cracking of high-density polyethylene, Eng. Fract. Mech. 203 (2018) 32.
24. ASTM G7/G7M Standard Practice for Atmospheric Environmental Exposure Testing of Nonmetallic Materials, 2011.
25. B.J. Briscoe, S.K. Sinha. Scratch resistance and localized damage characteristics of polymer surfaces-a review, Materialwissenschaft und Werkstofftechnik 34 (2003) 989.
26. P. Kurkcu, L. Andena, A. Pavan. An Experimental Investigation of the Scratch Behaviour of Polymers: 1. Influence of Rate-dependent Bulk Mechanical Properties, Wear 290-291 (2012) 86.
27. J. Hale, R. Lewis, M.J. Carré. Rubber friction and the effect of shape, Trib. Int. 141 (2020) 105911